

## Influence of projectile breakup in the elastic scattering of the ${}^{6,7}\text{Li}+{}^{80}\text{Se}$ systems

L. Fimiani<sup>1</sup>, J. M. Figueira<sup>1,2</sup>, G. V. Martí<sup>1,a</sup>, J. E. Testoni<sup>1</sup>, A. Arazi<sup>1,2</sup>, O. A. Capurro<sup>1</sup>, W. H. Z. Cárdenas<sup>1</sup>, M. A. Cardona<sup>1,2</sup>, P. Carnelli<sup>1,2,3</sup>, E. de Barbará<sup>1</sup>, D. Hojman<sup>1,2</sup>, D. Martinez Heimann<sup>1,2</sup>, A. E. Negri<sup>1,2</sup>, and A. J. Pacheco<sup>1,2</sup>

<sup>1</sup> Laboratorio Tandar, Comisión Nacional de Energía Atómica, B1650KNA San Martín, Buenos Aires, Argentina

<sup>2</sup> Consejo Nacional de Investigaciones Científicas y Técnicas, C1033AAJ Ciudad de Buenos Aires, Argentina

<sup>3</sup> Escuela de Ciencia y Tecnología, UNSAM, Campus Miguelete, B1650BWA San Martín, Buenos Aires, Argentina

**Abstract.** In order to study the influence of the breakup channel in the elastic scattering of the  ${}^{6,7}\text{Li}+{}^{80}\text{Se}$  systems, we have measured angular distributions at center-of-mass energies from  $13 \leq E_{c.m.} \leq 24$  MeV ( $0.8V_{CB}$  up to  $1.6V_{CB}$ ). They were analyzed within the framework of the optical model to study the energy dependence of the real and imaginary parts of the nuclear potential. The focus was to investigate the threshold anomaly in those weakly bound systems. The behavior of the calculated potentials as a function of energy indicates that our results are consistent with the dispersion relation. The threshold anomaly was observed in the  ${}^7\text{Li}+{}^{80}\text{Se}$  system and the breakup threshold anomaly was confirmed for the  ${}^6\text{Li}+{}^{80}\text{Se}$  system.

### 1 Introduction

The production of radioactive beams, has enabled the investigation of the dynamics and the structure of nuclei far from the stability line and it has also made possible to recreate nuclear reactions of astrophysical interest. When they are used to induce nuclear reactions there exists in general a large probability of breakup, giving rise to interesting effects comparing with the results obtained with bound systems, in which breakup processes are less common. Radioactive beams have low intensities, thus making experiments very difficult and time consuming to obtain statistically significant experimental data.

The use of beams of the stable  ${}^6\text{Li}$ ,  ${}^7\text{Li}$  and  ${}^9\text{Be}$  weakly bound nuclei to study the role played by the breakup channel has increasingly become a subject of interest in heavy-ion research [1, 2]. The separation energies of  $\alpha$ -particles for the breakup of  ${}^6\text{Li}$  and  ${}^7\text{Li}$ , are  $S_{\alpha}({}^6\text{Li})=1.47$  MeV and  $S_{\alpha}({}^7\text{Li})=2.47$  MeV, on account of these properties those stable nuclei have enhanced breakup probabilities and, therefore, they are particularly suitable for studying the breakup process and its influence on other reactions mechanisms.

The aim of this work is to investigate the influence of the breakup of  ${}^{6,7}\text{Li}$  projectiles on a relatively medium-mass target  ${}^{80}\text{Se}$  ( $Z=34$ ,  $N=46$ , intermediate between  ${}^{27}\text{Al}$  and  ${}^{144}\text{Sm}$ , already studied by our group [3–5]) throughout the behavior of the optical potentials deduced from the experimental measured elastic scattering angular distributions. A very preliminary report of this work was presented in [6]. A similar data analysis to that carried out by Figueira *et al.* [3–5] is proposed here. The objective is to obtain a set of potentials that should be able to give the best de-

scription of the above mentioned angular distributions. We have focused the analysis on the presence or absence of the threshold anomaly and breakup threshold anomaly [7, 8].

This report is organized as follows: Sec. 2 briefly describes the experimental setup and presents the experimental results. Follows Sec. 3 devoted to discuss the results of the theoretical analysis. Sec. 4 summarizes the entire work, discusses the conclusions and provides suggestions for future work to be carried out on this subject.

### 2 Experimental setup and results

Beams of  ${}^{6,7}\text{Li}$  were supplied by the 20 UD TANDAR accelerator on  ${}^{80}\text{Se}$  targets,  $110 \mu\text{g}/\text{cm}^2$  thick. The detection system consisted of an array of eight surface barrier detectors. The angular distributions were measured in steps of  $2.5^\circ$  covering an angular range of  $\approx 160^\circ$ . For additional details on the experimental setup and details see Refs. [6, 9]. The experimental elastic scattering cross sections (normalized to Rutherford cross section) plotted as a function of the scattering angle for the  ${}^{6,7}\text{Li}+{}^{80}\text{Se}$  systems are shown in Figs. 1 and 2 for  ${}^6\text{Li}+{}^{80}\text{Se}$  and  ${}^7\text{Li}+{}^{80}\text{Se}$  systems respectively.

### 3 Optical model calculations

We discuss in what follows the results of the analysis of the elastic scattering cross sections using a phenomenological optical model potential. We evaluate its behavior as a function of energy at the sensitivity radius.

<sup>a</sup> e-mail: marti@tandar.cnea.gov.ar

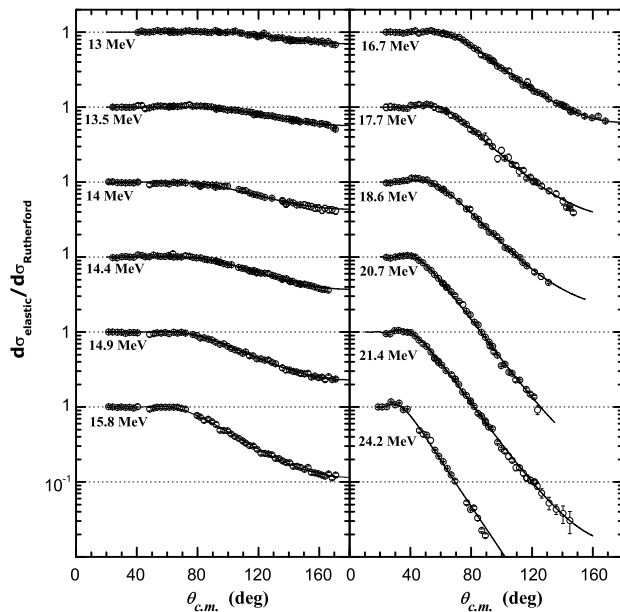


**Fig. 1.** Experimental elastic scattering cross sections normalized to the Rutherford cross sections for the  ${}^6\text{Li}+{}^{80}\text{Se}$  system (open circles and their best fits from optical model calculations (solid lines). Energies are given in the center of mass frame.

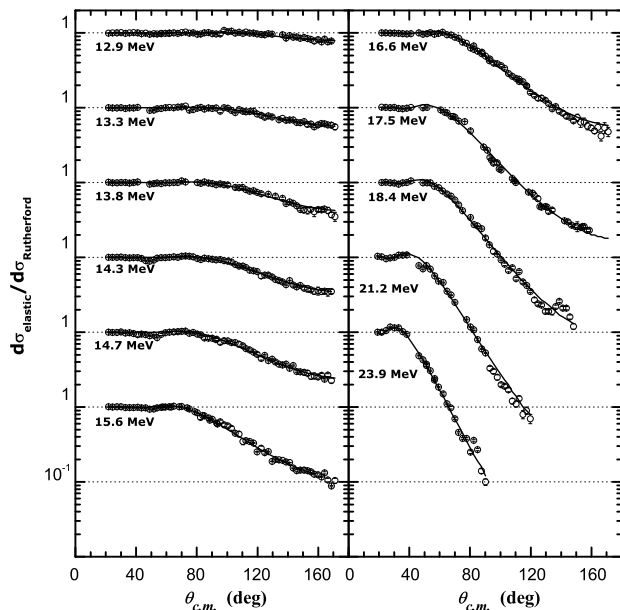


**Fig. 2.** Experimental elastic scattering cross sections normalized to the Rutherford cross sections for the  ${}^7\text{Li}+{}^{80}\text{Se}$  system (open circles and their best fits from optical model calculations (solid lines). Energies are given in the center of mass frame.

The phenomenological potential is defined as follows:

$$U(r) = V_C(r) - Vf(r) - iW_v f(r) - iW_s g(r), \quad (1)$$

where the first term represents the Coulomb potential, the second term is the real nuclear potential and the third and fourth terms are a volume and a surface absorptive imaginary potential, respectively. The usual Woods-Saxon form factor and its derivative were adopted for  $f(r)$  and  $g(r)$

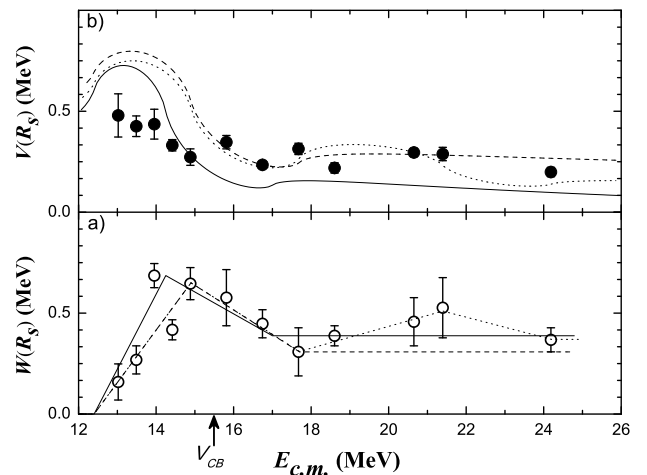


**Fig. 3.** a) Imaginary (open circle) and b) real (full circle) parts of the optical potentials, as a function of the center of mass energy, evaluated at the sensitivity radius, for the  ${}^6\text{Li}+{}^{80}\text{Se}$  system. The sensitivity radius  $R_s=10.4$  fm was taken as an average of the obtained values at different energies. The Coulomb barrier energy is displayed as a vertical arrow.

having the usual dependence in terms of the reduced radii and the diffuseness parameters. The parameters  $V$ ,  $W_v$  and  $W_s$  are the depths of the different contributions to the optical potential. The surface imaginary potential takes into account the absorption from peripheral processes (inelastic scattering and breakup) that occur mainly at distances close to  $r_C$ , while the volume imaginary potential describes the absorption from fusion. The angular distribution data for the elastic scattering of  ${}^{6,7}\text{Li}+{}^{80}\text{Se}$  systems were analysed searching for sets of optical model parameters that minimize the value of  $\chi^2/\text{point}$ . A first set of geometrical parameters was proposed based on the best fits calculated at the highest bombarding energies, namely 23 MeV and 26 MeV. The values of the geometrical parameters were the same for both systems, namely  $r=r_{W_s}=1.25$  fm,  $r_{W_v}=1.0$  fm,  $a=a_{W_s}=0.75$  fm and  $a_{W_v}=0.3$  fm. The reduced radius for the Coulomb term was fixed at  $r_C=1.1$  fm. These geometrical parameters were kept fixed throughout the calculations and were constrained to  $r_{W_v} \leq r=r_{W_s}$  and  $a=a_{W_s}$ . In this way it was taken into account the fact that in the fusion processes both the projectile and target nucleus have to come close enough to overcome the Coulomb repulsion and to get attracted by the short-range nuclear force. The calculations and the analysis was mainly concentrated in obtaining the optical potential strengths  $V$ ,  $W_v$  and  $W_s$  that best describe the experimental data. They were performed with the code PTOLEMY [10] and the obtained results are summarized in Fig. 3 and discussed in what follows.

For  ${}^6\text{Li}+{}^{80}\text{Se}$ , Fig. 3a) shows that the imaginary part of the optical potential at the sensitivity radius  $W(R_s)$ , is approximately constant up to  $E_{c.m.} \geq 17$  MeV. Below that energy, it increases as the energy decreases to reach a maximum at approximately 14 MeV, then it decreases sharply and almost vanishes at the lowest measured energy. The fact that the imaginary part of the potential continues to increase even as the energy decreases below the barrier suggests

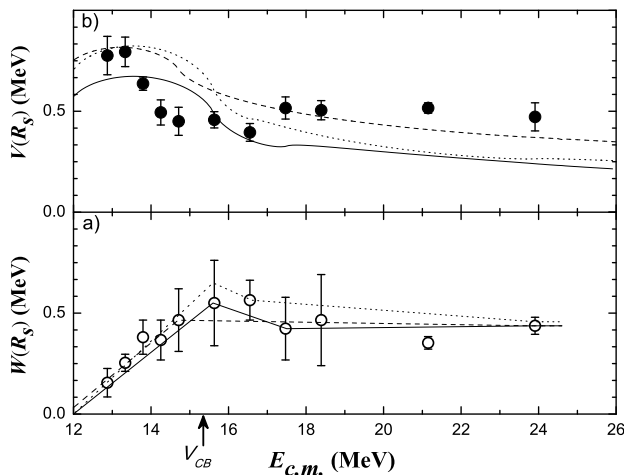


**Fig. 4.** a) Imaginary (open circle) and b) real (full circle) parts of the optical potentials, as a function of the center of mass energy, evaluated at the sensitivity radius, for the  ${}^7\text{Li}+{}^{80}\text{Se}$  system. The sensitivity radius  $R_s=10.2$  fm was taken as an average of the obtained values at different energies. The Coulomb barrier energy is displayed as a vertical arrow.

that inelastic and/or breakup channels remain open in this sub-barrier region, in contrast with the behavior observed for tightly-bound systems where the threshold anomaly is found. Fig. 3 b) shows the behavior of the real component  $V(R_s)$  of the optical potential. Above the barrier energy, it remains constant, while below the barrier it increases as the energy decreases up to almost twice the value at the barrier. The experimental points are compared with the results of the calculations obtained through the dispersion relation based upon the corresponding series of linear segments shown in Fig. 3 a). A qualitative agreement between the experimental data and the theoretical calculations indicates that the dispersion relation is satisfied for this system.

For the  ${}^7\text{Li}+{}^{80}\text{Se}$  system, (see Fig. 4 a)) the imaginary component  $W(R_s)$  is relatively energy independent above the Coulomb barrier and it decreases below the barrier as energy decreases. On the other hand,  $V(R_s)$  (see Fig. 4 b)) is also rather constant as a function of energy above the Coulomb barrier energy. Then, correlated with the imaginary potential through the dispersion relation (see the dotted, dashed and full lines in Fig. 4 a)), it increases with decreasing energy developing an approximate bell-shape behavior. Taking the real and the imaginary parts of the optical potentials together, these behaviors are consistent with the ordinary threshold anomaly usually observed in tightly bound systems [11].

## 4 Summary and conclusions

We have reported measurements of the elastic scattering angular distributions for the  ${}^{6,7}\text{Li}+{}^{80}\text{Se}$  systems at bombarding energies from below to above the nominal Coulomb barrier. An optical model analysis based upon  $\chi^2$ -minimization using a Woods-Saxon phenomenological potential was carried out. For the case of the elastic scattering of  ${}^7\text{Li}$  the behav-

ior of the real and imaginary parts of the optical potential as a function of energy is compatible with the presence of the threshold anomaly. On the other hand the behavior of the imaginary part of the phenomenological potential strongly suggest the absence of the TA or the presence of the BTA. The results for the elastic scattering of  ${}^{6,7}\text{Li}+{}^{80}\text{Se}$  systems confirm the qualitative agreement with the relation dispersions.

Comparing the scattering of  ${}^6\text{Li}$  and  ${}^7\text{Li}$  nuclei by several targets, an almost overall behavior for  ${}^6\text{Li}$  is much more clearly compatible with the BTA than for  ${}^7\text{Li}$ . The reason for that might be the higher breakup threshold energy for  ${}^7\text{Li}$  and the fact that for this nucleus there is a competition between the repulsive breakup polarization potential [12] and the attractive polarization potential produced by its first excited bound state [13]. To qualitatively evaluate the influence of breakup relative to inelastic channels coupled-channel calculations and/or continuous discretized coupled-channel calculations should be carried out in the future.

Some of us acknowledge the financial support of CONICET, CNEA and SECyT.

## References

1. D. M. Heimann *et al.*, Proceedings of International Conference on New Aspects of Heavy Ion Collisions Near the Coulomb Barrier (FUSION08), Chicago, 2008, AIP Conf. Proc. **1098-1**, (2009) 275.
2. L. F. Canto *et al.*, Phys. Rep. **424**, (2006) 1.
3. J. M. Figueira *et al.*, Phys. Rev C **73**, (2006) 054603.
4. J. M. Figueira *et al.*, Phys. Rev C **75**, (2007) 017602.
5. J. M. Figueira *et al.*, Phys. Rev C **81**, (2010) 024613.
6. L. Fimiani *et al.*, Phys. Rep. **424**, (2006) 1.
7. G. R. Satchler, Phys. Rep. **199**, (1991) 147.
8. M. S. Hussein *et al.*, Phys. Rev. C **73**, (2006) 044610.
9. D. Abriola *et al.*, Nucl. Instr. and Meth. B **268**, (2010) 1793.
10. M. H. Mcfarlane *et al.*, ANL internal report **76-11**, (1978).
11. D. Abriola *et al.*, Phys. Rev. C **39**, (1989) 546.
12. J. Lubian *et al.*, Nucl. Phys. A **791**, (2007) 24.
13. J. Lubian *et al.*, Phys. Rev. C **64**, (2001) 027601.